New results from the NA57 experiment

Presented by G.E. Bruno for the NA57 Collaboration:

F. Antinori[l], P.A. Bacon[e], A. Badalà[g], R. Barbera[g], A. Belogianni[a], A. Bhasin[e], I.J. Bloodworth[e], M. Bombara[j], G.E. Bruno[b], S.A. Bull[e], R. Caliandro[b], M. Campbell[h], W. Carena[h], N. Carrer[h], R.F. Clarke[e], A. Dainese[l], A.P. de Haas[s], P.C. de Rijke[s], D. Di Bari[b], S. Di Liberto[o], R. Divia[h], D. Elia[b], D. Evans[e], K. Fanebust[c], F. Fayazzadeh[k], G.A. Feofilov[q], R.A. Fini[b], P. Ganoti[a], B. Ghidini[b], G. Grella[p], H. Helstrup[d], M. Henriquez[k], A.K. Holme[k], A. Jacholkowski[b], G.T. Jones[e], P. Jovanovic[e], A. Jusko[i], R. Kamermans[s], J.B. Kinson[e], K. Knudson[h], A.A. Kolozhvari[q], V. Kondratiev[q], I. Králik[i], A. Kravčáková[j], P. Kuijer[s], V. Lenti[b], R. Lietava[f], G. Løvhøiden[k], V. Manzari[b], G. Martinská[j], M.A. Mazzoni[o], F. Meddi[o], A. Michalon[r], M. Morando[l], E. Nappi[b], F. Navach[b], P.I. Norman[e], A. Palmeri[g], G.S. Pappalardo[g], B. Pastirčák[i], J. Pišút[f], N. Pisutova[f], F. Posa[b], E. Quercigh[l], F. Riggi[g], D. Röhrich[c], G. Romano[p], K. Šafařík[h], L. Šándor[h,i], E. Schillings[s], G. Segato[l], M. Senè[m], R. Senè[m], W. Snoeys[h], F. Soramel[l], M. Spyropoulou-Stassinaki[a], P. Staroba[n], T.A. Toulina[q], R. Turrisi[l], T.S. Tveter[k], J. Urbán[j], F.F. Valiev[q], A. van den Brink[s], P. van de Ven[s], P. Vande Vyvre[h], N. van Eijndhoven[s], J. van Hunen[h], A. Vascotto[h], T. Vik[k], O. Villalobos Baillie[e], L. Vinogradov[q], T. Virgili[p], M.F. Votruba[e], J. Vrláková[j] and P. Závada[n]

[a] *Physics Department, University of Athens, Athens, Greece*
[b] *Dipartimento IA di Fisica dell'Università e del Politecnico di Bari and INFN, Bari, Italy*
[c] *Fysisk Institutt, Universitetet i Bergen, Bergen, Norway*
[d] *Høgskolen i Bergen, Bergen, Norway*
[e] *University of Birmingham, Birmingham, UK*
[f] *Comenius University, Bratislava, Slovakia*
[g] *University of Catania and INFN, Catania, Italy*
[h] *CERN, European Laboratory for Particle Physics, Geneva, Switzerland*
[i] *Institute of Experimental Physics, Slovak Academy of Science, Košice, Slovakia*
[j] *P.J. Šafárik University, Košice, Slovakia*
[k] *Fysisk Institutt, Universitetet i Oslo, Oslo, Norway*
[l] *University of Padua and INFN, Padua, Italy*
[m] *Collège de France, Paris, France*
[n] *Institute of Physics, Prague, Czech Republic*
[o] *University "La Sapienza" and INFN, Rome, Italy*
[p] *Dipartimento di Scienze Fisiche "E.R. Caianiello" dell'Università and INFN, Salerno, Italy*
[q] *State University of St. Petersburg, St. Petersburg, Russia*
[r] *Institut de Recherches Subatomique, IN2P3/ULP, Strasbourg, France*
[s] *Utrecht University and NIKHEF, Utrecht, The Netherlands*

We report results from the experiment NA57 at CERN SPS on hyperon production at midrapidity in Pb-Pb collisions at 158 A GeV/c and 40 A GeV/c. Λ, Ξ and Ω yields are compared with those from the STAR experiment at the higher energy of the BNL RHIC. Λ, Ξ, Ω and preliminary K^0_S transverse mass spectra are presented and interpreted within the framework of a hydro-dynamical blast wave model.

1 Introduction

The NA57 experiment has been designed to study the onset of enhanced production of multi-strange baryons and anti-baryons in Pb-Pb collisions with respect to p-Be collisions. This enhancement, first observed by experiment WA97 [1], is considered as evidence [2] for a phase transition to a new state of matter – the Quark Gluon Plasma (QGP).
The assessment of the combined results of the CERN heavy-ion experiments suggests indeed that a colour deconfined new state of matter [3] is produced in central Pb-Pb collisions at 158 A GeV/c.
NA57 has extend the study initiated by its predecessor WA97 by investigating the dependence of the hyperon production *(i)* on the interaction volume and *(ii)* on the collision energy per incoming nucleon [4]. For the first purpose, special efforts were made in NA57 to enlarge, with respect to WA97, the triggered fraction of the total inelastic cross-section thus extending the centrality range towards less central collisions; for the second, the experiment has collected data at two beam momenta: 158 A GeV/c and 40 A GeV/c.

2 The NA57 experiment

The NA57 apparatus has been described in detail elsewhere [5]. Strange and multi-strange hyperons are identified by reconstructing their weak decays into final states containing only charged particles, e.g.: $\Xi^- \rightarrow \Lambda\pi^-$, with $\Lambda \rightarrow p\pi^-$. Tracks are measured in the silicon telescope, an array of pixel detector planes with 5×5 cm^2 cross section, having a total length of about 30 cm. To improve the momentum resolution of high momentum tracks an array of double-sided silicon microstrip detectors is placed downstream of the tracking telescope. The whole silicon telescope is placed inside a 1.4 Tesla magnetic field, above the beam line, inclined and aligned with the lower edge of the detectors laying on a line pointing back to the target. The inclination angle α with respect to the beam line and the distance d of the first pixel plane from the target are varied with the beam momentum so as to accept particles produced in about half a unit of rapidity at central rapidity and medium transverse momentum, namely: at 158 A GeV/c ($y_{cm} \simeq 2.9$) $\alpha = 40$ mrad and $d = 60$ cm, at 40 A GeV/c ($y_{cm} \simeq 2.2$) $\alpha = 72$ mrad and $d = 40$ cm.
An array of scintillation counters, placed 10 cm downstream of the target, provides a fast signal to trigger on the centrality of the collisions. The centrality of the Pb-Pb collisions is determined (off-line) by analyzing the charged particle multiplicity measured by two stations of silicon strip detectors which cover, respectively, the pseudorapidity intervals $2 < \eta < 3$ and $3 < \eta < 4$ for the 158 A GeV/c set-up, and $2 < \eta < 3$ and $2.4 < \eta < 3.7$ for the 40 A GeV/c one. At both energies the triggered fraction of the total nuclear inelastic cross section is about 60%.
In order to estabilish whether in Pb-Pb interactions the multi-strange particle production is enhanced with respect to the superposition of elementary hadronic interactions, reference data are necessary. NA57 has collected p-Be data at 40 GeV/c (whose analysis is ongoing), while as reference data at 158 GeV/c we use both the p-Be and the p-Pb sets of data available from the WA97 experiment.

3 Data analysis

The hyperon signals are extracted with a method similar to that used in the WA97 experiment [6]. For each particle species we tune the optimal choice of the fiducial acceptance window using a Monte Carlo simulation of the apparatus. The data are then corrected for geometrical acceptance and for detector and reconstruction inefficiencies on a particle-by-particle basis, as described in references [7,8]. The stability of the results (inverse slopes and extrapolated yields, see later) is checked with respect to different choices of the acceptance window.

Finally we determine the double differential cross section $\frac{d^2N}{dm_T dy}$ — where y is the *rapidity* and $m_T = \sqrt{p_t^2 + m_0^2}$ is the *transvers mass* of the particle of rest mass m_0 — and the number of particles per event, i.e. the yield, in the selected acceptance window. The double differential cross section can be parametrized according to the following expression:

$$\frac{d^2N}{dm_T dy} = A\, m_T \exp\left(-\frac{m_T}{T_{app}}\right) \tag{1}$$

where the parameter T_{app}, which is referred to as the *inverse slope* (see section 5 for its physical interpretation), is extracted by means of a maximum likelihood fit method. By using the parametrization of eq. 1 we can extrapolate the yield measured in the selected acceptance window to a common phase space window covering full p_T and one unit of rapidity centered at midrapidity:

$$Yield = \int_m^\infty \mathrm{d}m_T \int_{y_{cm}-0.5}^{y_{cm}+0.5} \mathrm{d}y \frac{d^2N}{\mathrm{d}m_T \mathrm{d}y}. \tag{2}$$

As a measure of the collision centrality we use the number of wounded nucleons, i.e. the nucleons which take part in the initial collisions [9].
At 158 A GeV/c the multiplicity distribution is divided into five centrality classes $(0, I, II, III, IV)$[a], class 0 being the most peripheral and class IV the most central. The average number of wounded nucleons $< N_{wound} >$ in each class is determined from the trigger cross section, as described in reference [10].
At 40 A GeV/c, the results on hyperon yields are given and compared to those at higher energy for a single centrality class corresponding approximately to the most central 42% of the Pb-Pb interaction cross section, which is the equivalent of bins from I to IV at 158 A GeV/c.

4 Hyperon yields

4.1 Energy dependence

The yields for the Λ, Ξ^-, Ω^- hyperons and their anti-hyperons are shown in fig. 1 at the two beam energies. Going from 40 to 158 A GeV/c, the Λ and Ξ^- yields are quite similar while

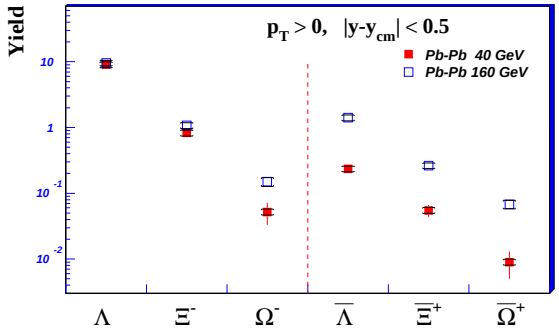

Figure 1: Particle yields in 40 and 158 A GeV/c Pb-Pb interactions, for about the 42% most central collisions.

the yields of the corresponding anti-particles are increased by a factor ~ 5. The Ω hyperon production shows a larger increase: about a factor 3 for the particle and more than a factor 7 for the anti-particle. This picture indicates, as expected, a larger baryon density at lower energy.

[a] The labels I-IV were introduced by WA97. The NA57 most peripheral bin is indicated with symbol 0 to keep the labelling of WA97 for the other centrality bins.

This trend continues when going from SPS to RHIC: in fig. 2 the NA57 yields are compared with those obtained in $\sqrt{S_{NN}}$ = 130 GeV Au-Au collisions from the STAR experiment at RHIC [11,12,13] (NA57 data points at 40 and 160 A GeV/c correspond to $\sqrt{S_{NN}}$ = 8.8 and 17.3 GeV, respectively). In order to stay close to the STAR range of collision centrality (5%, 10% and 14% most central Au-Au collisions for Λ, Ξ and Ω, respectively) we restrict here our centrality range to the 5% most central Pb-Pb collisions (class IV) in the case of Λ and to the 12% most central ones (classes III, IV) for Ξ and Ω. The Λ and Ξ^- yields stay almost constant all along

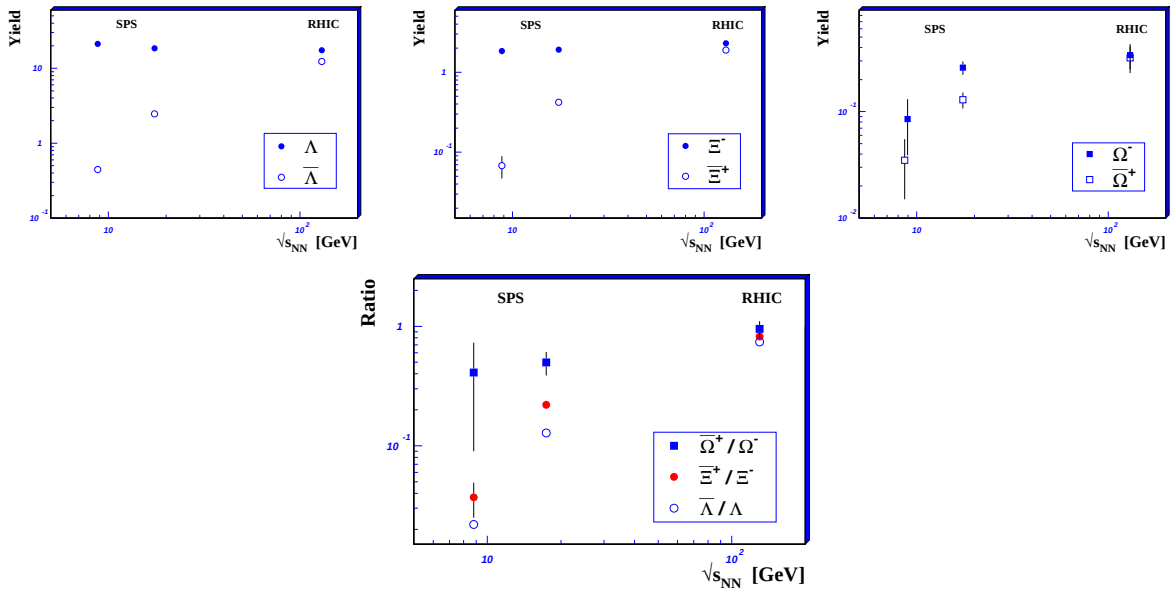

Figure 2: Comparison of strange particle yields (top) and anti-hyperon to hyperon ratios (bottom) at SPS and RHIC energies.

the full energy range, whereas an increase with the energy is observed for the Ω^- particle. All the three anti-hyperon yields show a much stronger increase with the energy.
From the yields, the ratios between the abundances of different particles can be computed. In particular, the anti-hyperon/hyperon ratios at SPS and RHIC are larger for higher strangeness content of the hyperon (bottom plot of fig. 2). All three hyperon ratios also increase as a function of the energy. Finally, the energy dependence is found to be weaker for particles with higher strangeness content.

4.2 Centrality dependence at 158 A GeV/c

In fig.3 the yields per wounded nucleon relative to p-Be of Λ, Ξ and Ω and their anti-particles in Pb-Pb and p-Pb at 158 A GeV/c are plotted as a function of the number of wounded nucleons. The p-Be and p-Pb results are those published by WA97. The particles have been divided into two classes, those with at least one valence quark in common with the nucleon (left) and those without (right), since it is known that the particles of two groups may exhibit different production features, e.g. in the rapidity spectra.
The NA57 results confirm the pattern of strangeness enhancements observed by WA97: when going from p-Be to Pb-Pb data, Ω are more enhanced than Ξ, which are in turn more enhanced than Λ. The maximum enhancement is about a factor 20 for the $\Omega^- + \overline{\Omega}^+$ in the most central class.
From fig. 3 one can see, within the Pb-Pb sample, an increase of the particle yields per wounded nucleon with the number of wounded nucleons for all the particles except for the $\overline{\Lambda}$.

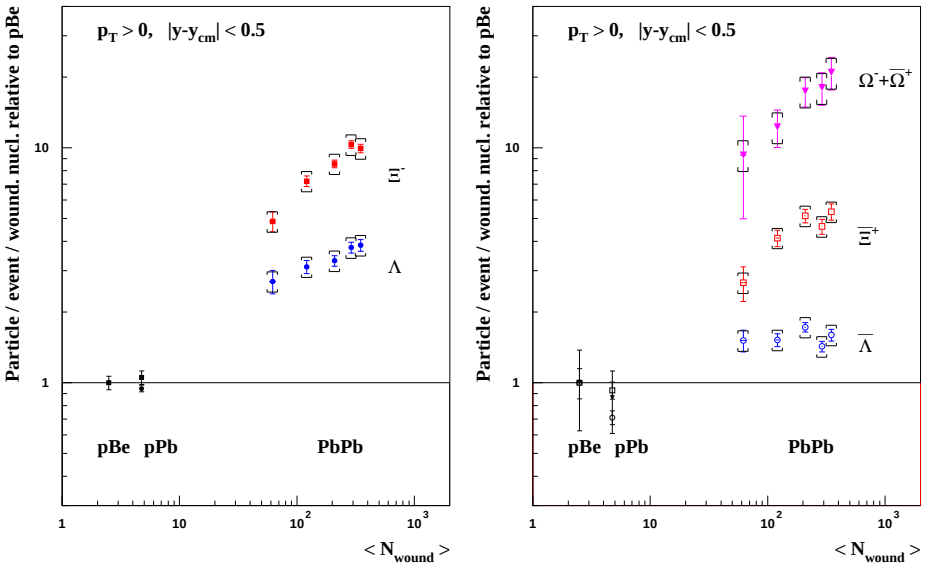

Figure 3: Hyperon yields per wounded nucleon per unit of rapidity at central rapidity relative to p-Be as a function of the number of wounded nucleons. The symbol ⊓⊔ indicates the systematic error.

5 Transverse mass spectra at 158 A GeV/c

In fig. 4 all the transverse mass spectra of the measured hyperons and anti-hyperons and (preliminary) K^0_S are collected. This sample corresponds to 54% most central Pb-Pb collisions. The values of the inverse slope parameters, as calculated according to maximum likelihood fits with the function of eq. 1 (see section 3) are reported in table 1.

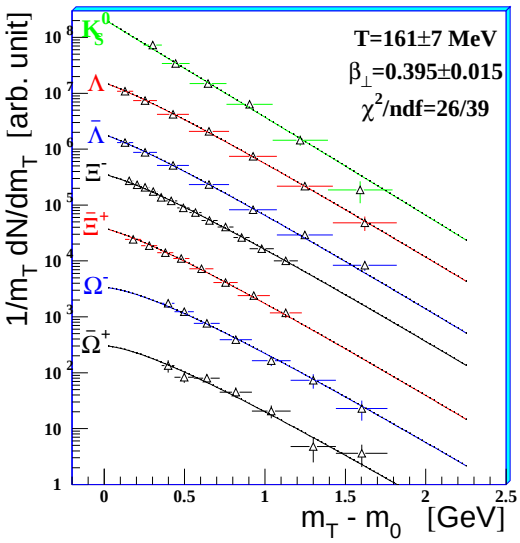

Figure 4: Transverse mass spectra of the strange particles measured by NA57 with superimposed the result of the best fit with the blast wave model.

Assuming a collective transverse expansion superimposed to the thermal motion of a fireball locally in thermal equilibrium, in two extreme regimes — namely non-relativistic ($p_T \ll m_0$) and ultrarelativistic ($m_T \gg m_0$) — the inverse slope parameter T_{app} can be simply related to two basic quantities: the thermal freeze-out temperature **T** and the (average) collective transverse flow velocity $\beta_\perp$. In the former regime one should expect an increase of T_{app} with the rest mass

Table 1: Inverse slopes parameter (T_{app}) of the strange particles in the full centrality range (**0-IV**).

Particle	K^0_S	Λ	$\overline{\Lambda}$	Ξ^-	$\overline{\Xi}^+$	Ω^-	$\overline{\Omega}^+$
T_{app} **(MeV)**	229 ± 9	289 ± 7	287 ± 9	297 ± 5	316 ± 11	280 ± 16	324 ± 29

of the particles: e.g. in reference [14] it has been derived that $T_{app} = \mathbf{T} + m_0 < {\beta_\perp}^2 >$; in the latter regime the inverse slope parameter would be just blue-shifted with respect to $\mathbf{T}$ according to a Doppler formula [15]: $T_{app} = \mathbf{T}\sqrt{\frac{1+\beta_\perp}{1-\beta_\perp}}$.
For the description of the full m_T region we have employed here the hydro-dynamical model derived in reference [15]. In its simplest interpretation, when a constant transverse velocity profile is assumed, the transverse mass distribution becomes:

$$\frac{d^2N}{m_T dm_T dy} \propto m_T K_1\left(\frac{m_T cosh\rho}{\mathbf{T}}\right) I_0\left(\frac{p_T sinh\rho}{\mathbf{T}}\right) \tag{3}$$

where $\rho = tanh^{-1}\beta_\perp$ and K_1 and I_0 are two modified Bessel functions. A simultaneous best fit of eq. 3 to the data points of all the measured strange particle spectra successfully describes all the distributions with $\chi^2/ndf = 26.3/39$, yielding the following values for the two basic quantities $\mathbf{T}$ and $\beta_\perp$:

$$\mathbf{T} = 161 \pm 7 MeV\,, \qquad \beta_\perp = 0.395 \pm 0.015\,.$$

The particles have been divided again in two groups — those which share quarks in common with the nucleons and those which do not — and the fit procedure has been repeated separately for the two groups. The results of such fits are summarized in table 2. They suggest common

Table 2: Thermal freeze-out temperature T and average transverse flow velocity $\beta_\perp$ in the full centrality range.

particles	$\mathbf{T}$ (MeV)	$\beta_\perp$	χ^2/ndf
K^0_S, Λ, Ξ^-	160 ± 10	0.39 ± 0.02	12.7/15
$\overline{\Lambda}$, $\overline{\Xi}^+$, Ω^- , $\overline{\Omega}^+$	167 ± 16	0.39 ± 0.03	12.2/22

freeze-out conditions for the two groups. Since the interaction cross-sections for the particles of the two groups are quite different, this finding would suggest a similar production mechanism and limited importance final state interactions (e.g. a sudden thermal freeze-out). A similar conclusion concerning the evolution of the system was reached in the paper by WA97 studying the HBT correlation functions of negative pions [16].
Finally, we have attempted to study the centrality dependence. We present here very preliminary results for three different centralities only, in order to reduce the statistical error: our (5%) most central collision class IV, classes 0 and I merged (most peripheral group) and classes II and III merged (intermediate centrality). In table 3 are reported the fit parameters and the centrality ranges in terms of residual percentage of the total inelastic cross-section. The suggested trend is as follows: the more central the collisions the larger the transverse collective flow and the lower the final thermal freeze-out temperature. The higher temperature for peripheral collisions could be due to the shorter time duration of the expansion: the sytem would have less time for cooling before of the final decoupling. The results for our most central class are consistent within the errors with those in the same centrality range from a similar analysis by NA49 [17].

Table 3: Thermal freeze-out temperature T and average transverse flow velocity $\beta_\perp$ as a function of centrality.

Centrality	**T** (MeV)	$\beta_\perp$	χ^2/ndf
0-I $23 \div 54\%$	163 ± 16	0.35 ± 0.03	37.8/37
II-III $5 \div 23\%$	167 ± 13	0.40 ± 0.03	32.6/37
IV $0 \div 5\%$	131 ± 10	0.47 ± 0.02	37.4/37

6 Conclusions and outlook

Results from NA57 on Λ, Ξ and Ω production in Pb-Pb collisions at both 40 and 158 A GeV/c have been reported. The energy dependence of the hyperon and anti-hyperon yields is compatible with a decrease of the baryon density with increasing energy. Going from low (40 A GeV/c) to top (158 A GeV/c) SPS beam momentum the Λ and Ξ^- yields stay roughly constant while the production of the Ω^- and all the anti-hyperons increases significantly with the collision energy; this trend continues up to the RHIC energy. At 158 A GeV/c the centrality dependence of the yields per wounded nucleon confirms the pattern of enhancements relative to p-Be observed by WA97: the enhancement increases with the strangeness content of the particle, up to a factor ≈ 20 for $\Omega^- + \overline{\Omega}^+$. All the particles except the $\overline{\Lambda}$ show an increase of the enhancements, when going from peripheral to central Pb-Pb collisions: a saturation may be possible for the two – three most central bins. The ongoing data analysis on p-Be collisions will soon provide results on the pattern of strange particle enhancements at 40 A GeV/c.
The preliminary analysis of the transverse mass spectra at 158 A GeV/c in the framework of a hydro-dynamical model with a constant velocity profile suggests that after the collision the system expands explosively, with a tranverse velocity of about one half of the speed of light; the system then freezes-out when the temperature is of the order of 150 MeV. Finally the preliminary results on the centrality dependence of the expansion dynamics indicate that with increasing centrality the transverse flow velocity increases and the final temperature decreases.

References

1. R.A. Fini *et al.*, *J. Phys. G: Nucl. Phys.* **27**, 375 (2001).
   F. Antinori *et al.*, *Nucl. Phys.* A **661**, 130c (1999).
2. J. Rafelski and B. Müller, *Phys. Rev. Lett.* **48**, 1066 (1982).
3. U. Heinz and M. Jacob, nucl-th/0002042 (2000) and reference therein
   see also http://www.cern.ch/CERN/Announcements/2000/NewStateMatter.
4. R. Caliandro *et al.*, NA57 Proposal, CERN/SPSLP 96-40, SPSLC/P300.
5. T. Virgili *et al.*, *Nuclear Physics* A **681**, 165 (2001).
6. I. Kralik *et al.*, *Nucl. Phys.* A **638**, 5c (1998).
7. G.E. Bruno *et al.*, Proceedings of The XXXVIIth Rencontres de Moriond, March 17th-24th 2002, hep-ex/0207047.
8. V. Manzari *et al.*, *Nucl. Phys.* A **715**, 140c (2003).
9. C.Y. Wong in *Introduction to High-Energy Heavy-Ion Collisions* (World Scientific, Singapore, 1994) p 251 , and references therein.
10. N. Carrer *et al.*, *J. Part. Phys. G: Nucl. Part. Phys.* **27**, 391 (2001).
11. C. Adler *et al.*, *Phys. Rev. Letters* **89**:092301 (2002).
12. J. Castillo *et al.*, nucl-ex/0211032 (2002).
13. C. Suire *et al.*, nucl-ex/0211017 (2002).
14. U. Heinz, preprint nucl-th/9801050 (1998).
15. E. Schnedermann, J. Sollfrank and U. Heinz, *Phys. Rev.* C **48**, 2462 (1994).

16. F. Antinori *et al.*, *J. Part. Phys. G: Nucl. Part. Phys.* **27**, 2325 (2001).
17. M. Van Leeuwen *et al.*, *Nucl. Phys.* A **715** (2003), nucl-ex/0208014.